Numerical simulation of the electromagnetic instability of an intense beam in a quadrupole focusing system

J. Krall, C. M. Tang, and T. Swyden*
Beam Physics Branch, Plasma Physics Division, Naval Research Laboratory, Washington, D.C. 20375-5320
(Received 10 April 1992; revised manuscript received 25 June 1992)

Discrete quadrupole focusing systems are subject to an electromagnetic instability wherein the growing transverse motion of the beam interacts with the quadrupole field and the TE_{11} waveguide mode. We study this via three-dimensional particle simulation. We find evidence of the instability, with growth rates and frequencies in reasonable agreement with theory. The instability is found to saturate at a low amplitude, however, and has no discernable effect on the macroscopic properties of the beam.

PACS number(s): 41.75.Ht, 41.85.Ja

I. INTRODUCTION

Discrete quadrupole focusing systems, also called FODO lattices (for focusing field, zero field, defocusing field, zero field), have been used to transport charged particle beams for a variety of applications. In Ref. [1], we showed that FODO-lattice transport systems are subject to an electromagnetic instability wherein growing transverse perturbations of an electron beam result from the interaction of the beam with the FODO-lattice field and a TE_{11} waveguide mode. This instability is analgous to that observed in helical quadrupole transport systems [2–5].

Specifically, we consider an alternating-gradient quadrupole field (B_{qx}, B_{qy}), where

$$B_{qx} = -B_q k_q \cos(nk_q z) y \ , \tag{1a}$$

$$B_{qy} = -B_q k_q \cos(nk_q z) x \ , \tag{1b}$$

$B_q k_q$ is the peak field gradient, $k_q = 2\pi/\lambda_q$, and λ_q is the period of the quadrupole field. In Ref. [1], the dispersion relation for the instability was derived and numerical solutions were presented. It was found that for given parameters, peak growth rates occur at a single frequency but with multiple wave numbers. It was also found that secondary modes exist, again with multiple wave numbers at each frequency, but with significantly lower growth rates. Finally, it was shown that the primary mode is "cutoff" for a small enough waveguide radius or low enough beam energy. Results were also in agreement with those of Ref. [6].

As an example, an (ω, k) diagram is given in Fig. 1 for a case in which the quadrupole gradient is $B_g k_q = 1000$ G/cm, the wave number is $k_q = 0.55$ cm^{-1}, the waveguide radius $r_g = 3$ cm, and $\gamma = 7$, where γ is the usual relativistic factor for the beam. For clarity, the diagram corresponds to the limit of zero beam current. In Fig. 1, the primary mode occurs at points indicated by a circle. Secondary modes occur where an unstable beam mode (straight line) intersects a waveguide mode (curved line) other than the primary mode. These are indicated by squares. Figure 2 shows the temporal growth rate of the primary instability $\mathrm{Im}(\omega/c)$ plotted versus wave number for the parameters of Fig. 1, but with beam current $I_b = 2$ kA. These figures, which are obtained by numerically solving Eq. (23) of Ref. [1], show the periodic

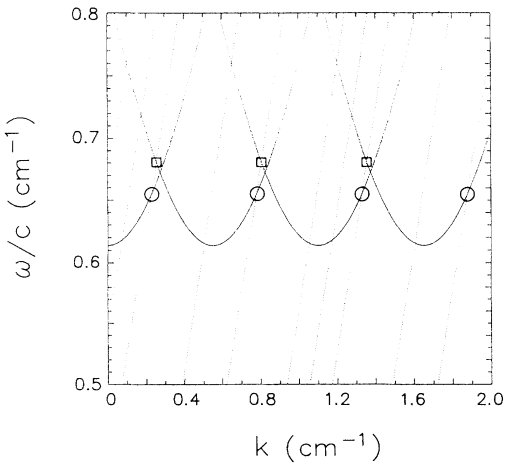

FIG. 1. Dispersion diagram in the low-current limit. The primary instability occurs at points indicated by circles. A secondary instability occurs at points indicated by squares.

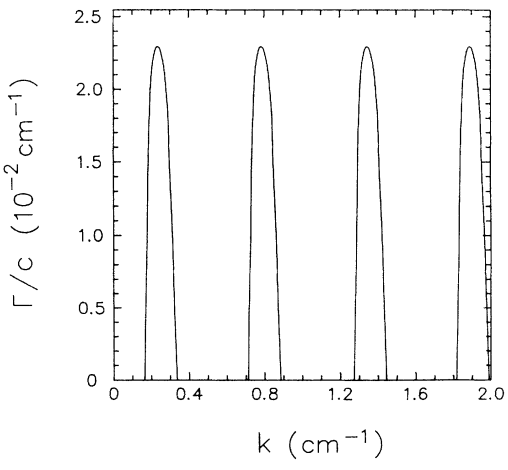

FIG. 2. Temporal growth rate of the primary mode for $\omega > 0$ as a function of wave number k for parameters listed in Table I, case *C*.

nature of the instability.

This paper was motivated by the desire to numerically investigate this instability, which (according to the analysis) is nearly unavoidable for long-pulse (>10 ns), high-current (>100 A), moderate-energy (<100 MeV) electron beams.

II. NUMERICAL RESULTS

Simulations were performed using the ELBA [7] computer code. ELBA is a three-dimensional particle code which simulates a beam propagating within a cylindrical metallic pipe. The full set of Maxwell's equations along with the full relativistic motion of the beam particles are included.

For each simulation, initial particle positions and velocities were "matched" to the FODO field in the envelope sense as in Ref. [8], including an *ad hoc* correction for space charge. For comparison to the ELBA runs, simulations were also performed using the SST [9] code. The SST code is a single-slice version of the ELBA code which assumes no variation in the beam along the axial direction. Because the axial derivatives are dropped, the SST code cannot exhibit the instability. This allowed us to distinguish physical effects (current loss, emittance growth, etc.) that may be caused by the instability from those that arise from imperfections in the matching scheme (see, e.g., Ref. [10]).

Growth rates were measured by analyzing the TE_{11} mode, for which the B_z and E_r components may be "projected out" from the electromagnetic spectrum in a straightforward manner. Because our simulation takes place in a coordinate system that moves with the beam $(r,\theta,\zeta=ct-z)$, these growth rates are $\Gamma/c=\mathrm{Im}(\omega/c-k)$. This corresponds to the theoretical result only in the case that $\mathrm{Im}(k)=0$ as was assumed in numerically solving the dispersion relation.

Simulations were performed for parameters typical of a high-current, induction-accelerator beam, $I_b=1$–2 kA, $\gamma_0=7$, and normalized rms emittance $\epsilon_{n,\mathrm{rms}}=0.05$–$0.16$ cm rad. Simulation parameters are listed in Table I. In a typical run, a beam of length $L_b=250$ cm was transported over 10 m in the presence of the external focusing fields. It was not practical to simulate a case in which the primary mode is cut off, as given by Eq. (33) of Ref. [1]. For the parameters of Fig. 2, for instance ($B_q k_q=1000$ G/cm, $k_q=0.55$ cm^{-1}, $r_g=3$ cm, $I_b=2$ kA, and $\gamma=7$), this would require either a reduction in beam energy to $\gamma<1.4$ or a reduction in the waveguide radius to $r_g<0.43$ cm.

In each run, we found a growing TE_{11} mode as predicted by theory, but without a growing displacement of the beam centroid. In fact, the instability saturated at a low level, apparently due to mode competition between the various wave numbers and, possibly, between the primary and secondary modes.

TABLE I. Simulation parameters. Other beam parameters were $\gamma=7$ and $\epsilon_{n,\mathrm{rms}}=0.16$ cm rad for the $I_b=1$ kA cases and $\epsilon_{n,\mathrm{rms}}=0.05$ cm rad for the $I_b=2$ kA cases.

Run	I_b (kA)	$k_q B_q$ (G/cm)	k_q (cm^{-1})	r_g (cm)
A	1.0	200	0.60	3.0
B	1.0	200	0.40	3.0
C	2.0	1000	0.55	3.0
D	2.0	1000	0.55	4.0

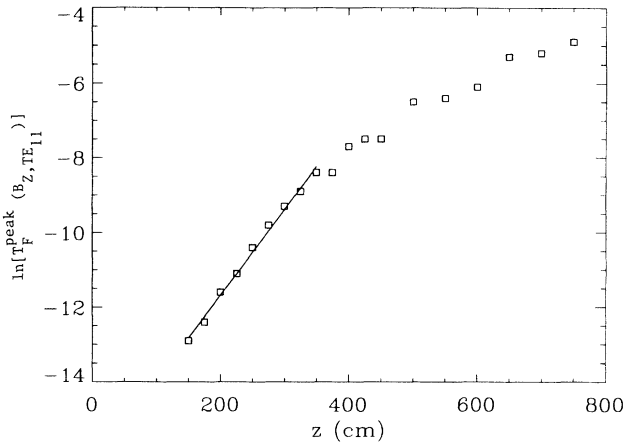

FIG. 3. The natural logarithm of the peak of the Fourier transform, in frequency space, of the B_z component of the TE_{11} mode vs propagation distance for the $B_q k_q=1000$ G/cm, $r_g=3.0$ cm case (case *C* in Tables I and II). A linear least-squares fit to the first nine points is also plotted.

As an example, we return to the parameters of Fig. 2. Here, we simulated an $L_b=250$ cm, $I_b=2$ kA, $\gamma=7$, $\epsilon_{n,\mathrm{rms}}=0.05$ cm rad beam propagating for 10 m. The following were observed.

(1) As the TE_{11} mode grew, the peak frequency of the spectrum shifted continuously. Exponential growth rates could only be obtained by plotting the logarithm of the peak of the Fourier transform of the TE_{11} mode versus propagation distance z, as in Fig. 3. The points in Fig. 3 show approximately linear growth over the first 300 cm of propagation with growth rate $\Gamma/c=0.023$ cm^{-1} and frequency $\omega/c=0.58\pm0.12$ cm^{-1}. Theoretical values for this case are $\Gamma/c=0.024$ cm^{-1} and frequency $\omega/c=0.67\pm0.04$ cm^{-1}, where we are quoting the half

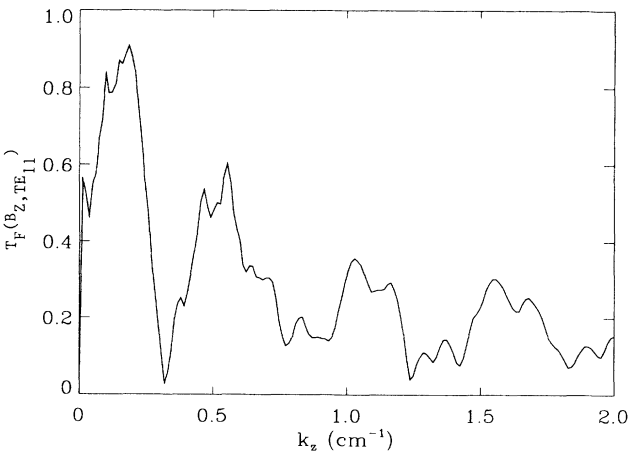

FIG. 4. Wave-number spectrum at $ct=175$ cm.

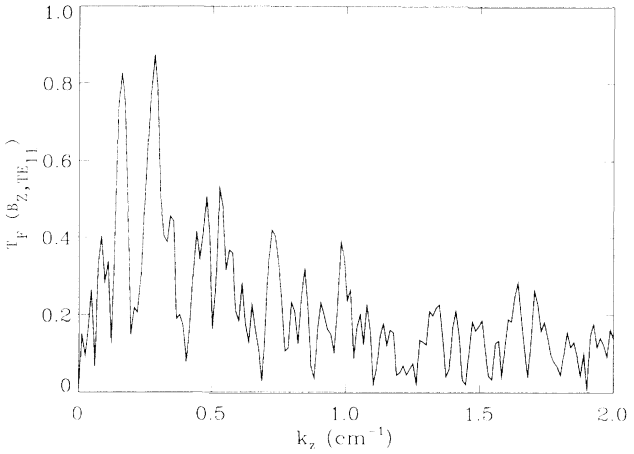

FIG. 5. Wave-number spectrum at $ct=1000$ cm.

width at half maximum of the Γ/c vs ω/c curve as the expected frequency spread.

(2) Early in the simulation the wave-number spectrum, shown in Fig. 4, resembled that expected from Fig. 2. At later times the spectrum is broadband. This is shown in Fig. 5.

(3) No net displacement of the beam centroid was observed. In fact, the instability had no discernable effect on the macroscopic parameters of the beam. One parameter that did evolve over the course of the simulation was the emittance, which grew as a result of imperfections in the initial match of the beam to the external fields. This growth was from $\epsilon_{n,\mathrm{rms}}=0.05$ to 0.20 cm rad. In an SST run with identical parameters, emittance grew from $\epsilon_{n,\mathrm{rms}}=0.05$ to 0.13 cm rad. It is not clear whether the difference in emittance growth between the ELBA and SST runs is caused by the instability or by differing particle statistics between the two codes. The latter is likely, however, as the final emittance in the SST code was reduced somewhat (10%) when the number of particles was doubled.

Results for all runs are summarized in Table II. For comparison, theoretical growth rates and frequencies, from numerical solutions of Eq. (23) of Ref. [1], are also shown. The $B_q k_q=1000$ G/cm, $r_g=4.0$ cm case, run *D*, was interesting in that the peak frequency of the TE$_{11}$-mode spectrum clearly jumped between the primary instability at $\omega/c=0.50\pm0.03$ cm^{-1}, and a higher frequency $\omega/c=0.64\pm0.02$ cm^{-1}. The value listed in Table II for this case, $\omega/c=0.54\pm0.07$ cm^{-1}, reflects a weighted average of these two frequencies. The higher frequency appears to correspond to the secondary mode at $\omega/c=0.67$ cm^{-1}. From numerical solutions of the dispersion relation, the secondary mode should have a growth rate $\Gamma/c<0.002$ cm^{-1} and, therefore, was not expected to play a role in these simulations.

TABLE II. Theoretical values of peak linear growth rate Γ/c and frequency ω/c and corresponding simulation results. Simulation growth rates for runs *A* and *B* could not be determined reliably because of the TE$_{11}$ mode was largely masked by particle "noise" in those cases. Growth rates and frequencies are in units of cm^{-1}.

	Theory		Simulation	
Run	Γ/c	ω/c	Γ/c	ω/c
A	0.0057	0.62±0.01		0.63±0.03
B	0.0069	0.71±0.02		0.55±0.07
C	0.024	0.67±0.03	0.023	0.58±0.12
D	0.021	0.50±0.01	0.027	0.54±0.07

III. CONCLUSIONS

An electromagnetic instability on an intense beam in a FODO lattice was studied via numerical simulation. We found evidence of the instability, with growth rates and frequencies in reasonable agreement with theory. The instability, however, was found to saturate at a low level, with field amplitudes two orders of magnitude lower than those observed in the helical quadrupole case. It has no discernable effect on the macroscopic properties of the beam.

This result is in sharp contrast to the corresponding instability in helical quadrupole fields. With helical quadrupole fields, the instability has been observed in simulations [2,4] and in experiments [5] to be extremely disruptive to beam transport.

We also find that the instability is broadband in both frequency and wave number. We speculate that significant mode competition is occurring both among the various unstable wave numbers of the primary instability and, possibly, between the primary instability and the higher-frequency secondary instability. The results suggest that the secondary instability may play a role in the growth of the primary instability despite the fact that its theoretical growth rate is more than an order of magnitude below that of the primary instability.

ACKNOWLEDGMENTS

We would like to thank T. P. Hughes and D. Chernin for helpful discussions. This work was supported by the Defense Advanced Research Projects Agency, Arpa Order No. 7781, the Strategic Defense Initiative Organization/Innovative Science and Technology Office, and the Office of Naval Research.

*Present address: FM Technologies, Inc., Fairfax, VA 22032.

[1] C. M. Tang, J. Krall, and T. Swyden, Phys. Rev. A **45**, 7492 (1992).

[2] T. P. Hughes and B. B. Godfrey, Phys. Fluids **29**, 1698 (1986).

[3] C. M. Tang, P. Sprangle, J. Krall, P. Serafim, and F. Mako, Part. Accel. **35**, 101 (1991).

[4] J. Krall, C. M. Tang, G. Joyce, and P. Sprangle, Phys. Fluids B **3**, 204 (1991).

[5] M. G. Tiefenback, S. D. Putnam, V. L. Bailey, Jr., J. P. Lidestri, and J. A. Edighoffer, Pulse Sciences, Inc. Report No. PSIFR-2543-01, 1991 (unpublished); T. P. Hughes, T. C. Genomi, K. Nguyen, and D. Welch, Mission Research Corp. Report MRC/ABQ-OR-1442, 1991 (unpublished).
[6] T. P. Hughes and D. Chernin (unpublished).
[7] G. Joyce, J. Krall, and S. Slinker, LANL Report No. LA-11857-C, 99, 1990 (unpublished).
[8] S. Humphries, *Charged Particle Beams* (Wiley, New York, 1990), Chap. 4.
[9] J. Krall, G. Joyce, and S. Slinker (unpublished).
[10] S. Slinker, G. Joyce, J. Krall and M. Lampe (unpublished).